Holzforschung, Vol. xx, pp. xxx-xxx, 2011 • Copyright © by Walter de Gruyter • Berlin • Boston. DOI 10.1515/HF.2011.127

Automatic grain texture analysis using integral transforms

Wayne Hall[1,*], Andrew Seagar[1] and Stuart Palmer[2]

[1] Griffith School of Engineering, Gold Coast Campus, Griffith University, Queensland, Australia
[2] Institute of Teaching and Learning, Deakin University, Waterfront Campus, Geelong, Victoria, Australia

*Corresponding author.
Griffith School of Engineering, Gold Coast Campus, Griffith University, Queensland 4222, Australia
E-mail: w.hall@griffith.edu.au

Abstract

Tonewood for musical instruments is quarter-sawn and frequently quality-graded based on visual appearance, mechanical and acoustic properties. The assessment uses simple human (subjective) observation, and two "experts" can rate the same sample differently. This paper describes the application of integral transforms (Fourier and Radon) for automatic (objective) assessment of the visual appearance of 10 Sitka spruce (*Picea sitchensis*) sample images. This work considers surface classification on the basis of grain orientation, count, spacing, and evenness or uniformity.

Keywords: Fourier transform; grain texture analysis; image processing; Radon transform; Sitka spruce.

Introduction

The term "tonewood" describes a wood with consistent acoustic qualities. Tonewood for musical instruments is quarter-sawn and frequently "quality-graded" based on the criteria of visual appearance, mechanical and acoustic properties (sound response). It is well established that elastic and strength properties are higher in the grain direction than perpendicular to the grain (Green 2001) and the elastic constants (i.e., elastic and shear moduli and Poisson ratios) are related to the resonant frequencies or eigen frequencies. The spectrum of these resonant frequencies and their relative strengths govern the resultant sound pitch and timbre of the wood (Wegst 2008), whilst internal friction (related to sustain or length of the sound) can be related to the width of the resonant peaks (Wei and Kukureka 2000). The density is related to the fibre length and diameter, lumen diameter, and cell wall thickness, whilst ray dimensions influence sonic velocity (Longui et al. 2010) and hence acoustic quality.

There is considerable research focus on physical measurement of those woods used in musical instrument construction (e.g., Schimleck et al. 2009), but, in practice, visual appearance seems to be the main criterion for soundboard quality-grading decisions, rather than mechanical and acoustic properties (Buksnowitz et al. 2007). The visual appearance is symptomatic (but not an assurance) of mechanical and acoustic properties. The highest grades are usually allocated to samples with the most consistent colour and even grain pattern. These woods are also the most accurately quarter-sawn with less grain "run out". Assessment is based simply on subjective human observation, and two "experts" can rate the same sample differently. Several assessors are therefore needed to produce statistically meaningful and repeatable results of surface texture evaluation.

Image processing has the potential to provide automatic, objective, and cost-effective tonewood evaluations. Logs have been evaluated using image processing methods by Nilsson and Edlund (2005), whilst computer tomography has been used by Wei et al. (2009) to create three-dimensional reconstructions. Wood composites have been considered by Walther and Thömen (2009) and Eberhardt et al. (2009). Image analysis has also been used to quantify anatomical details such as vessel characteristics (Chen and Evans 2010) and vessel network (Hass et al. 2010). An evaluation of the change in appearance of lumber surfaces (illuminated from various directions) was described by Nakamura et al. (2010). Khalid et al. (2008) describe an automatic wood recognition system based on image processing, feature extraction, and artificial neural networks, whilst Yu et al. (2005) have considered texture orientation for species classification.

This paper focuses on surface assessment of Sitka spruce (*Picea sitchensis*) as a tonewood for piano, violin, and guitar soundboards. *Picea sitchensis* is the "most widely planted commercial tree species in the United Kingdom and Ireland" (McLean et al. 2010). The work addresses the issue of automatic visual assessment of tonewoods with a visible, regular striated pattern. However, the method is not limited to tonewood evaluations and could be applied more broadly after adaptation as a wood classification tool. Consideration is given to the feasibility of an automatic grain texture evaluation tool based on grain orientation, count, spacing, and evenness (or uniformity) – rather than defects. Most existing image-based characterisation systems for quality grading purposes tend to consider surface defect identification (for example, knots, cracks etc.) (Piuri and Scotti 2010). Image processing is performed here using Fourier and Radon transforms (Weeks 1996; Budd and Mitchell 2008). The work focuses on the development of image processing methods to improve automatic (objective) surface evaluation.

Materials and methods

Ten Sitka spruce (*Picea sitchensis*) panels (~60 mm × ~60 mm) were created from a B-grade quarter-sawn soundboard blank supplied by Guitar Woods, Australia (www.guitarwoods.com.au). Sitka spruce exhibits a straight grain, with annual rings of wider, lighter-coloured earlywood blending into a narrower band of dark-coloured

latewood (Harris 1984). B-grade blanks have obvious colour variation across their surface, and an irregular grain pattern and spacing. A reasonable degree of sample variation was deemed important in this feasibility study. To ensure a representative sample, no attempt was made to smooth the surface of the blank; it was investigated in its "as supplied" condition.

Panels were cut from selected regions, spanning the width of the blank. The 10 panels are referred to with their identification numbers (SI01–SI10). The panel selections were made at locations where human visual assessment of grain texture was possible. The panels were scanned as colour images at 600 pixels/inch (~236 pixels per cm) with a Hewlett-Packard HP Colour LaserJet CM1312MFP. The colour images were then cropped to 1200 pixels/rows (50.8 mm)×1200 pixels/columns (50.8 mm) to ensure square sample images of consistent dimensions. The cropped colour images were assessed visually by the authors. Two of the samples (SI04 and SI07) were considered to be at, or near, the limit of what the authors could evaluate under normal (office) lighting. After scanning, the authors agreed on all images to within an error of ±1 grain, except in the case SI04. The results for sample Image SI04 are therefore not reported. The retained cropped images were then converted to greyscale to yield high resolution 8-bit (256 greyscale) images. The grain orientations of seven (out of the 10) panels were aligned approximately vertically (i.e., $\theta = \sim 0°$), with three panels orientated at about 10° (clockwise) intervals from the vertical. Assuming positive angles are anticlockwise rotations, negative angles are anticlockwise (i.e., $\theta = \sim$-10°, $\theta = \sim$-20°, and $\theta = \sim$-30°). The retained sample images were analysed by Fourier and Radon transforms. All numerical analyses were performed using Matlab (a widely available commercial mathematical package from The Math Works Inc., Natick, MA, USA).

Fourier transform (FT)

The FT is a mathematical method that provides a description of a signal or waveform or image in terms of a set of sinusoidal (i.e., sine and cosine) components of different frequency (1/wavelength), phase (relative position) and amplitude (height). The FT is a common technique for image (spatial) filtering to reduce image noise and/or to sharpen blurred features in images (Weeks 1996). Here, the FT is also applied in the latter mentioned context to emphasise the wood texture.

For a square (digital) image $f(x,y)$ with $N \times N$ pixels, the FT $F(u,v)$ and its inverse can be implemented with the 2D discrete FT (DFT) pair, viz.:

$$F(u,v) = \frac{1}{N^2} \sum_{x=0}^{N-1} \sum_{y=0}^{N-1} f(x,y)\, e^{-j2\pi\left(\frac{ux}{N} + \frac{vy}{N}\right)} \quad \text{(1a)}$$

$$f(x,y) = \frac{1}{N^2} \sum_{u=0}^{N-1} \sum_{v=0}^{N-1} F(u,v)\, e^{j2\pi\left(\frac{ux}{N} + \frac{vy}{N}\right)} \quad \text{(1b)}$$

where u and v are the spatial frequencies of the sinusoidal components in the x- and y-directions measured in units of peaks(maxima)-per-inch (PPI) or peaks-per-centimetre.

An image and its transform both contain $N \times N$ values – no information is lost or destroyed. Moreover, a transform followed by the inverse (without filtering) recovers the original image exactly. The frequency component $F(0,0)$ represents the average value of the image. This is commonly referred to as the Direct Current (DC) component: a terminology that comes from electrical engineering.

Herein, the sample images were 1200×1200 pixels (2 inches square, digitised at 600 dpi). At this resolution, the FT produces frequency components up to 300 peaks(maxima)-per-inch, corresponding to 600 peaks(maxima)-per-sample PPS, i.e., the maximum frequency component in the x- and y-directions are obtained when $u = N/2$ and $v = N/2$, respectively. All the sample images were filtered with a band-pass filter. All frequency components were retained that lie between a lower and an upper band edge, whilst discarding all components outside. The band-pass filter for each sample image was selected from maximum and minimum grain spacing estimates (based on a manual count of pixels) – this band-filter information, for each sample image, is presented in Table 1. The greyscale sample image and corresponding filtered image of a "typical" sample (SI01) is presented in Figure 1a and b. Figure 1c and d show for comparison greyscale sample images for SI02 and SI03. In the following discussion, the mathematical procedure and results are illustrated based on SI01; sample-specific details are demonstrated based on other samples (including SI02 and SI03).

Table 1 Band-pass filters.

Sample image	Band-edge (pixels per sample)	
	Lower	Upper
SI01	19.5	60.5
SI02	14.5	45.5
SI03	24.5	60.5
SI04	Discarded	
SI05	14.5	60.5
SI06	24.5	50.5
SI07	24.5	60.5
SI08	24.5	55.5
SI09	24.5	55.5
SI10	29.5	60.5

Radon transform (RT)

The RT represents an image as the projections (or line integrals of all lines on the image matrix) along specific directions. It is useful

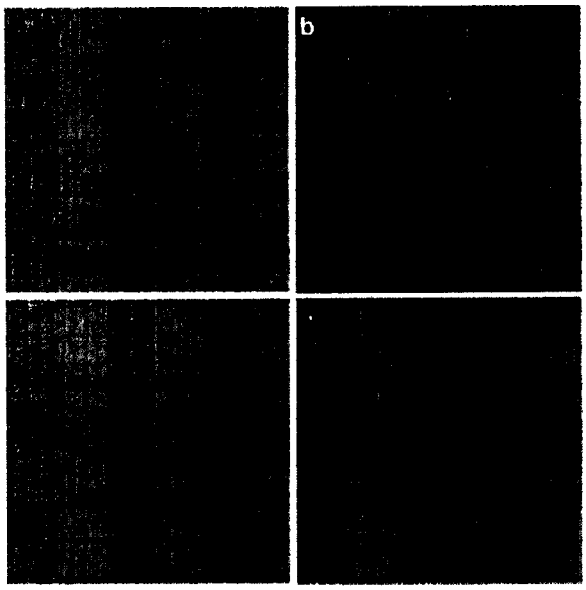

Figure 1 Typical images: (a) sample image SI01 (greyscale); (b) filtered image SI01; (c) sample image SI02 (greyscale) and (d) sample image SI03 (greyscale).

laurwood (Harris 1984). B-grade blanks have obvious colour variation across their surface, and an irregular grain pattern and spacing. A reasonable degree of sample variation was deemed important in this feasibility study. To ensure a representative sample, no attempt was made to smooth the surface of the blank; it was investigated in its "as supplied" condition.

Panels were cut from selected regions, spanning the width of the blank. The 10 panels are referred to with their identification numbers (SI01–SI10). The panel selections were made at locations where human visual assessment of grain texture was possible. The panels were scanned as colour images at 600 pixels/inch (~236 pixels per cm) with a Hewlett-Packard HP Colour LaserJet CM1312MFP. The colour images were then cropped to 1200 pixels/rows (50.8 mm)×1200 pixels/columns (50.8 mm) to ensure square sample images of consistent dimensions. The cropped colour images were assessed visually by the authors. Two of the samples (SI04 and SI07) were considered to be at, or near, the limit of what the authors could evaluate under normal (office) lighting. After scanning, the authors agreed on all images to within an error of ±1 grain, except in the case SI04. The results for sample Image SI04 are therefore not reported. The retained cropped images were then converted to greyscale to yield high resolution 8-bit (256 greyscale) images. The grain orientations of seven (out of the 10) panels were aligned approximately vertically (i.e., $\theta \approx 0°$), with three panels orientated at about 10° (clockwise) intervals from the vertical. Assuming positive angles are anticlockwise rotations, negative angles are anticlockwise (i.e., $\theta \approx -10°$, $\theta \approx -20°$, and $\theta \approx -30°$). The retained sample images were analysed by Fourier and Radon transforms. All numerical analyses were performed using Matlab (a widely available commercial mathematical package from The Math Works Inc., Natick, MA, USA).

Fourier transform (FT)

The FT is a mathematical method that provides a description of a signal or waveform or image in terms of a set of sinusoidal (i.e., sine and cosine) components of different frequency (1/wavelength), phase (relative position) and amplitude (height). The FT is a common technique for image (spatial) filtering to reduce image noise and/or to sharpen blurred features in images (Weeks 1996). Here, the FT is also applied in the latter mentioned context to emphasise the wood texture.

For a square (digital) image $f(x,y)$ with $N \times N$ pixels, the FT $F(u,v)$ and its inverse can be implemented with the 2D discrete FT (DFT) pair, viz.:

$$F(u,v) = \frac{1}{N^2} \sum_{x=0}^{N-1} \sum_{y=0}^{N-1} f(x,y)\, e^{-i2\pi\left(\frac{ux}{N} + \frac{vy}{N}\right)} \quad (1a)$$

$$f(x,y) = \frac{1}{N^2} \sum_{u=0}^{N-1} \sum_{v=0}^{N-1} F(u,v)\, e^{i2\pi\left(\frac{ux}{N} + \frac{vy}{N}\right)} \quad (1b)$$

where u and v are the spatial frequencies of the sinusoidal components in the x- and y-directions measured in units of peaks(maxima)-per-inch (PPI) or peaks-per-centimetre.

An image and its transform both contain $N \times N$ values – no information is lost or destroyed. Moreover, a transform followed by the inverse (without filtering) recovers the original image exactly. The frequency component $F(0,0)$ represents the average value of the image. This is commonly referred to as the Direct Current (DC) component, a terminology that comes from electrical engineering.

Herein, the sample images were 1200 × 1200 pixels (2 inches square, digitised at 600 dpi). At this resolution, the FT produces frequency components up to 300 peaks(maxima)-per-inch, corresponding to 600 peaks(maxima)-per-sample FPS, i.e., the maximum frequency component in the x- and y-directions are obtained when $u = N/2$ and $v = N/2$, respectively. All the sample images were filtered with a band-pass filter. All frequency components were retained that lie between a lower and an upper band edge, whilst discarding all components outside. The band-pass filter for each sample image was selected from maximum and minimum grain spacing estimates (based on a manual count of pixels) – this band-filter information, for each sample image, is presented in Table 1. The greyscale sample image and corresponding filtered image of a "typical" sample (SI01) is presented in Figure 1a and b. Figure 1c and d show for comparison greyscale sample images for SI02 and SI03. In the following discussion, the mathematical procedure and results are illustrated based on SI01; sample-specific details are demonstrated based on other samples (including SI02 and SI03).

Table 1 Band-pass filters.

Sample image	Band-edge (pixels per sample)	
	Lower	Upper
SI01	19.5	60.5
SI02	14.5	48.5
SI03	21.5	60.5
SI04	Discarded	
SI05	14.5	60.5
SI06	24.5	50.5
SI07	34.5	60.5
SI08	24.5	55.5
SI09	24.5	55.5
SI10	29.5	60.5

Radon transform (RT)

The RT represents an image as the projections (or line integrals of all lines on the image matrix) along specific directions. It is useful

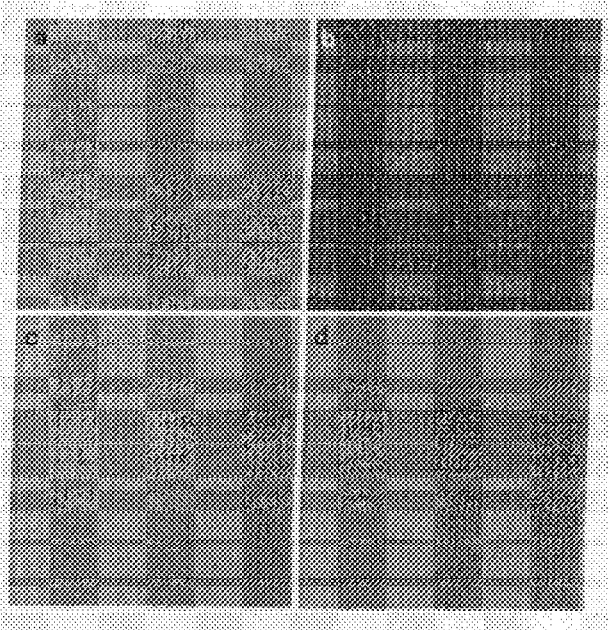

Figure 1 Typical images: (a) sample image SI01 (greyscale); (b) filtered image SI01; (c) sample image SI02 (greyscale) and (d) sample image SI03 (greyscale).

in line detection applications, including image processing, computer vision, and seismic applications (Zhang and Couloigner 2007). Its propensity for line detection makes it an ideal image analysis tool for studying wood grain texture (Yu et al. 2005). In this referenced work, consideration was given to grain texture orientation only. The feasibility of a full quantitative grain texture evaluation (as proposed here) is significantly more complex, especially on "as supplied" wood. The full texture evaluation considered in the present paper focuses on grain orientation, count, spacing, and uniformity.

The line integral for each line in a specific direction is:

$$R(L)=\int_L f(x,y)\,dy' \tag{2}$$

where $f(x,y)$ is the image and dy' is a small distance increment along the line length, L.

The straight lines pass through a series of points on the image. The lines are parallel to each other and are spaced at a constant increment, dx', apart. The points on each of the straight lines are at the constant increment, dy', along each of the line lengths. Their position can be defined relative to the x- and y-axes (located at the image centroid), or converted to the x'- and y'-coordinate system via:

$$(x,y)=(x'\cos\theta-y'\sin\theta, x'\sin\theta+y'\cos\theta) \tag{3}$$

The Radon transform of the image is obtained by substitution of Eq. (3) into Eq. (2), viz.:

$$R(x',\theta)=\int_L f(x'\cos\theta-y'\sin\theta, x'\sin\theta+y'\cos\theta)\,dy' \tag{4}$$

Results and discussion

Grain orientation

Radon transform projections were computed for a 90° range of angles ($-45° \le \theta \le 44°$) with a 0.1° interval. For each sample image, at each angle, the root sum square (RSS) of the line integrals was calculated. The grain orientation for each sample image was identified as the angle where the RSS value was maximum. The RSS plots for sample images SI01, SI08, SI09 and SI10 are shown in Figure 2. The RSS maxima on the plots correlate to the grain orientations as expected or measured (i.e., SI01 ~ 0°, SI08 ~ 10° clockwise, SI09 ~ 20° clockwise, and SI10 ~ 30° clockwise).

Grain count, spacing, and uniformity

The image projections at the grain orientation angles for sample images SI01–SI07 were calculated by RT. These are all orientated at approximately 0°; sample images SI08–SI10 were not assessed for grain count. Figure 3a shows the image projection of the sample image SI01 (presented in Figure 1a) at an angle of -0.6°. The modified image projection data for identifying the grain count are given in Figure 3b and c. The horizontal axis corresponds to the distance dx' from the centre of the sample image. The magnitude of the line integral (the sum of the intensities along dy') is plotted on the vertical axis.

The earlywood (EW) tends to yield positive values, whilst the negative values relate to the darker latewood (LW) (Figure 3a). These positive and negative values arise from

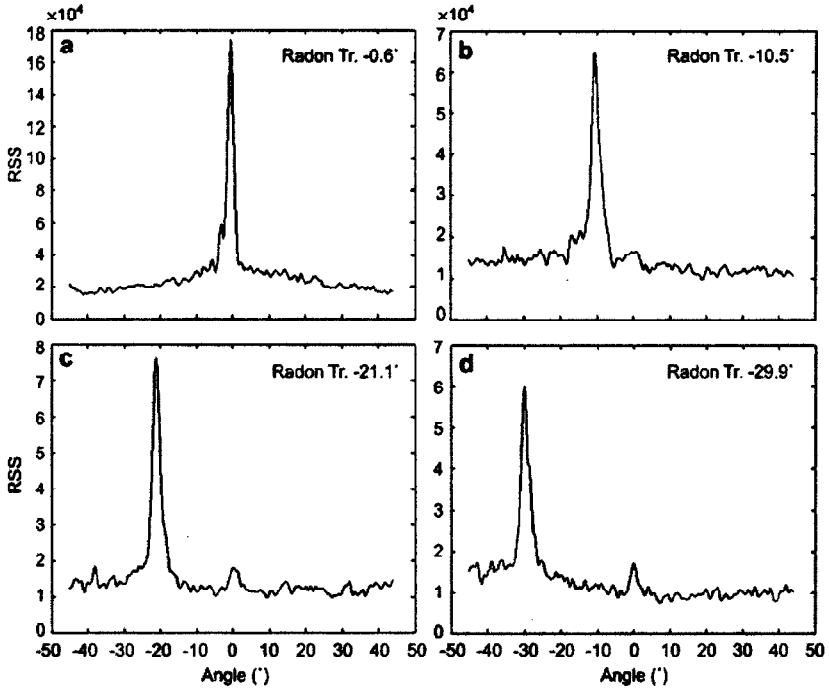

Figure 2 Grain orientation RSS plots: (a) SI01; (b) SI08; (c) SI09 and (d) SI10.

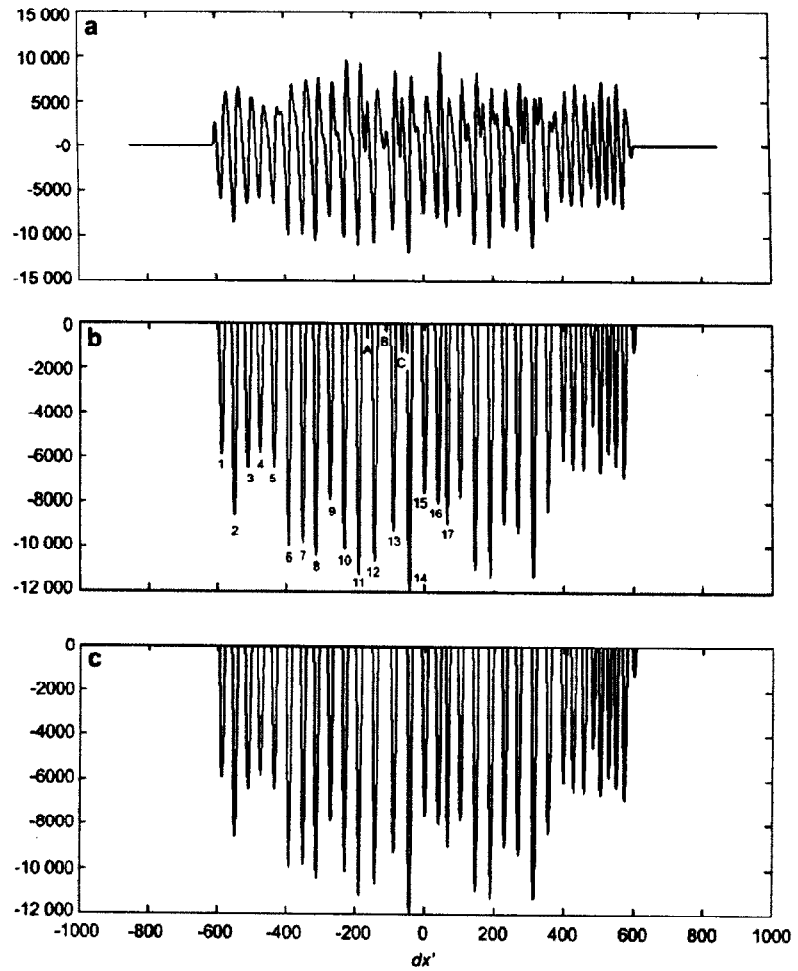

Figure 3 Grain count plots: (a) image projection; (b) modified projection and (c) after grain selection.

the filtering procedure, specifically the removal of the DC component. The grain count is identified from the number of LW occurrences and, hence, only the negative data are retained; the positive data are set to zero – Figure 3b. The peaks, evident in Figure 3b, include all visually identified LW occurrences (numbers 1–17 of 33 are shown), but further include some spurious occurrences (letters A–C). These arise from surface features that have not been removed during the Fourier filtering procedure. They are evident for most sample images after image processing has been completed and tend to have significantly lower amplitudes than the "true" LW signals. Based on the characteristics of the signal, an automatic grain selection process attempts to remove these spurious occurrences (Figure 3c).

The automatic grain selection process identifies all peaks in the negative data, both true and spurious. Peaks are then removed (considered to be anomalous) if they have a low magnitude by setting two noise thresholds. A low threshold is set at 10% of the magnitude of adjacent peak/s, a high threshold at 25%. Those with magnitudes lower than the 10% threshold are assumed to be inconsistent and instantly removed. The peaks with magnitudes between 10% and 25% are only removed if the distance between them and previous peaks is deemed to be "atypical". Atypical means: if the distance (period) between the current peak and the previous one is more than 1.5-times of that of the previous two periods, i.e., at variance to normal growth patterns. To ensure that no anomalous data are retained, the automatic selection process is repeated several times. Figure 3c demonstrates the outcome of the procedure. Spurious peaks have been identified and removed.

For comparison, the visual evaluation and automatic grain counts are listed in Table 2. Sample images with author agreement of ± 1 grain are compared. The visual and automatic evaluations for SI01, SI02, SI03, and SI07 are in agreement. All LW occurrences are correctly identified on sample images SI05 and SI06. Furthermore, the spurious peaks surrounded by true LW occurrences are all correctly removed. Some ambiguity remains at the edges of the sample, where both spurious and/or true LW occurrences can lead to small (but significant) peaks, if the grain boundaries are not perfectly aligned with the sample edges. This will vary from sample to sample, but it is the case for SI05 and SI06. Grain orientations for these two samples were -1.1°

Table 2 Comparison of visual and automatic grain count.

Sample image	Sample evaluation		Comment
	Visual	Automatic	
SI01	32 or 33	33	Correct
SI02	30	30	Correct
SI03	37	37	Correct
SI04	Discarded		–
SI05	32	33	All LW correct*
SI06	37	38	All LW correct*
SI07	37 or 38	37	Correct

*All latewood occurrence correctly identified.

and -0.8°, respectively. Such ambiguity is likely to be eliminated with proper alignment of the sample, or by visual and automatic assessment of a modified sample image. For example, a parallelogram (rather than a square or rectangular) image with two sides of the original sample image cropped at the computed grain orientation could be helpful in ensuring proper alignment.

For each sample image, pixel distances between LW occurrences (identified from the minimum peak values above – see Figure 3c) are easily determined. The mean, $\bar{x}$, and standard deviation, s, of these pixel distances can then be used as objective indicators of typical grain spacing (or to calculate grains per inch or cm etc.) and evenness (uniformity), respectively. Sample images SI02 and SI03 have significant differences in their grain spacing and uniformity and were taken here for illustration – see Figure 1c and d. SI02 has fewer grains than SI03, and they are spaced more widely apart on the left-hand side of the image with tighter grains presented on the right-hand side. The cause of this "spacing drift" is not addressed here, but could result from non-alignment through the thickness (i.e., the sample could have been incorrectly quartersawn). Confirmation would require evaluation of the tonewood's cross-section. In contrast, the grains for SI03 are much more evenly spaced, but show a degree of waviness (the grain is kinked). The mean and standard deviations quantify the significant differences in grain spacing for these two sample images, but can also be used to characterise similar samples that are more difficult to assess visually. The mean and standard deviations (in parentheses) are 40.2 (±7.8) pixels and 32.6 (±4.4) pixels for SI02 and SI03, respectively. Grain waviness is not part of this study, but it is postulated here that it could manifest itself as a distinct feature in the grain orientation (RSS) plots.

Conclusions

This paper describes the application of integral transforms (Fourier and Radon) for automatic wood surface classification. Grain orientation, count, spacing, and evenness (uniformity) were assessed from 600 dpi colour scanned images. The grain orientation was characterised for 1200×1200 pixel sample images by means of the root sum square (RSS) of the line integrals (after band-pass filtering). If the grain count can be visually identified from a colour scanned image, the integral transforms method can successfully identify the number of grains. Here, the grain count was identified from the number of latewood (LW) occurrences. It is proposed that mean and standard deviations of the pixel distances between these LW occurrences can be used as objective indicators of grain spacing and uniformity. These initial results demonstrate that Fourier and Radon transforms can be a practical tool for wood surface evaluation. Future work will consider automatic classification of soundboard blanks into relative grades of quality.

Acknowledgements

The authors would like to thank the referees for comments which have led to an improved manuscript.

References

Budd, C., Mitchell, C. (2008) Saving lives: the mathematics of tomography. Plus Magazine, No. 47 (available on-line at http://plus.maths.org/issue47/features/budd/, accessed 21/12/2010).

Buksnowitz, C., Teischinger, A., Muller, U., Pahler, A., Evans, R. (2007) Resonance wood [*Picea abies* (L.) Karst.] – Evaluation and prediction of violin makers' quality-grading. J. Acoustic Soc. America 121:2384–2395.

Chen, F.F., Evans, R. (2010) Automated measurement of vessel properties in birch and poplar wood. Holzforschung 64:369–374.

Eberhardt, T.L., So, C.-L., Protti, A., So, P.-W. (2009) Gadolinium chloride as a contrast agent for imaging wood composite components by magnetic resonance. Holzforschung 63:75–79.

Green, D.W. (2001) Wood: strength and stiffness. In: Encyclopedia of Materials: Science and Technology. Eds. Buschow, K.H.J., Chan, R.W., Flemings, M.C., Ilschner, B., Kramer, E., Mahajan, S., Vessiere, P. Elsevier, Amsterdam, The Netherlands. pp. 9732–9736.

Harris, A. (1984) Sitka Spruce. United States Department of Agriculture, FS-265 (available on-line at http://www.fpl.fs.fed.us/documnts/usda/amwood/265sitka.pdf, accessed 16/02/11).

Hass, P., Wittel, F.K., McDonald, S.A., Marone, F., Stampanoni, M., Herrmann, H.J., Niemz, P. (2010) Pore space analysis of beech wood: the vessel network. Holzforschung 64:639–644.

Khalid, M., Lee, E.L.Y., Yusof, R., Nadaraj, M. (2008) Design of an intelligent wood species recognition system. Int. J. Simul. Systems Sci. Techn. 9:9–19.

Longui, E.L., Lombardi, D.R., Alves, E.S. (2010) Potential Brazilian wood species for bows of string instruments. Holzforschung 64:511–520.

McLean, J.P., Evans, R., Moore, J.R. (2010) Predicting the longitudinal modulus of elasticity of Sitka spruce from cellulose orientation and abundance. Holzforschung 64:495–500.

Nakamura, M., Matsuo, M., Nakano, T. (2010) Determination of the change in appearance of lumber surfaces illuminated from various directions. Holzforschung 64:251–257.

Nilsson, D., Edlund, U. (2005) Pine and spruce roundwood species classification using multivariate image analysis on bark. Holzforschung 59:689–695.

Piuri, V., Scotti, F. (2010) Design of an automatic wood types classification system using flourescence spectra. IEEE Trans. Syst. Man Cyb. C: Applic. Rev. 20:358–366.

Schimleck, L.R., Espey, C., Mora, C.R., Evans, R., Taylor, A., Muniz, G. (2009) Characterization of the wood quality of pernambuco (*Caesalpinia echinata* Lam) by measurements of density, extractives content, microfibril angle, stiffness, color, and NIR spectroscopy. Holzforschung 63:457–463.

Walther, T., Thoemen, H. (2009) Synchrotron X-ray microtomography and 3D image analysis of medium density fiberboard (MDF). Holzforschung 63:581–587.

Weeks, A.R. (1996) Fundamentals of electronic image processing. Wiley-IEEE Press, Piscataway, NJ.

Wegst, U.G.K. (2008) Bamboo and wood in musical instruments. Ann. Rev. Mat. Res. 38:323–349.

Wei, C.Y., Kukureka, S.N. (2000) Evaluation of damping and elastic properties of composites and composite structures by the resonance technique. J. Mat. Sci. 35:3785–3792.

Wei, Q., Zhang, S.Y., Chui, Y.H., Leblon, B. (2009) Reconstruction of 3D images of internal log characteristics by means of successive 2D log computed tomography images. Holzforschung 63:575–580.

Yu, H., Liu, Y., Liu, Z. (2005) Auto detection of wood texture orientation by Radon Transform. J. Forestry Res. 16:1–4.

Zhang, Q., Couloigner, I. (2007) Accurate centreline detection and line width estimation of thick lines using the Radon transform. IEEE Trans. Image Process. 16:310–316.

Received February 23, 2011. Accepted June 24, 2011.